

## 69. Organic Reactions in the Solid State: The Reactivity of Guest Molecules in Tri-*o*-thymotide Clathrates

by Raymond Gerdil\* and Giacomo Barchietto

Department of Organic Chemistry, University of Geneva, CH-1211 Geneva 4

(27.XII.93)

---

Tri-*o*-thymotide (TOT) clathrates are enantiomorphous and enantioselective (chiral cages). It was shown that an external molecular reactant can diffuse into the TOT host crystal lattice and reacts with the included molecule (guest) in characteristic ways, differing from those occurring in liquid solutions. Several aspects of the action of hydrogen halides (HCl, HBr) on the chemical behavior of included oxiranes were investigated for solid-gas and solid-liquid (aqueous) systems. Under well established experimental conditions, these reactions gave regiospecifically one target product and were asymmetric. The included substrate underwent first an acid-catalyzed allylic isomerization that is cage-specific and mostly quantitative. In sheer contrast, strong basic conditions were required to promote, in reduced yield, the analogous transformation in solution. The regiospecificity and enantioselectivity of several intra-crystalline conversions allowed the accurate determination of the absolute configuration of several guest molecules. Kinetic measurements were achieved that disclosed some striking features of this new type of heterogeneous reactions. Tentative models for the cage stereoselective mechanisms are briefly discussed.

---

**1. Introduction.** – Clathrates are crystalline species formed by the inclusion of ‘guest’ molecules into cavities or channels generated by the packing of ‘host’ molecules. A main requirement is that no covalent bonds exist between host and guest molecules. Tri-*o*-thymotide<sup>1)</sup> (TOT, **1**) occupies a prominent place among the chiral hosts, owing to its ability to include a large number of guests of different natures and sizes [1]. The versatility of TOT as a host molecule is further exemplified by the discovery of clathrates belonging to thirteen different space groups, two of which being enantiomorphous (the host lattice of any single crystal consists entirely of the same TOT antipodes). The TOT clathrates of interest in this study belong to the space group  $P3_121$  and comprise closed dissymmetric cavities (*Fig. 1*), each cavity including a single guest molecule with no mutual contact possible between the guests<sup>2)</sup>. The cage dissymmetry endows the cages (receptors) with the property of discriminating between the enantiomers of a chiral guest (substrate), resulting in the preferential inclusion of one of the antipodes of a racemic mixture. On consideration that the clathrates recrystallize with spontaneous resolution, the separation of guest enantiomers is, therefore, potentially possible *via* this route. This property bears great significance in the present work.

We previously showed that an external reactant (<sup>1</sup>O<sub>2</sub>) can penetrate the clathrate crystal lattice and react with the guest with simultaneous transfer of chirality from the

---

<sup>1)</sup> 1,7,13-Trimethyl-4,10,16-tris(1-methylethyl)-6*H*,12*H*,18*H*-tribenzo[*b,f,j*][1,5,9]trioxacyclododecane-6,12,18-trione.

<sup>2)</sup> Unless otherwise stated, all clathrates mentioned herein are of the cage-type and belong to space group  $P3_121$ .

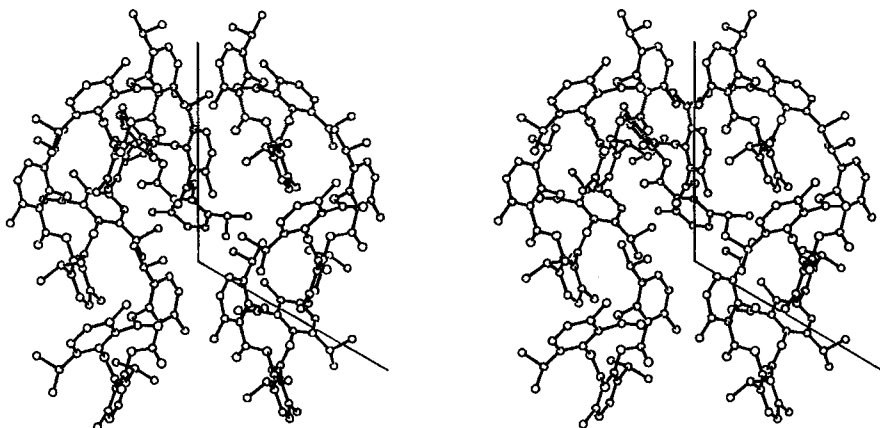
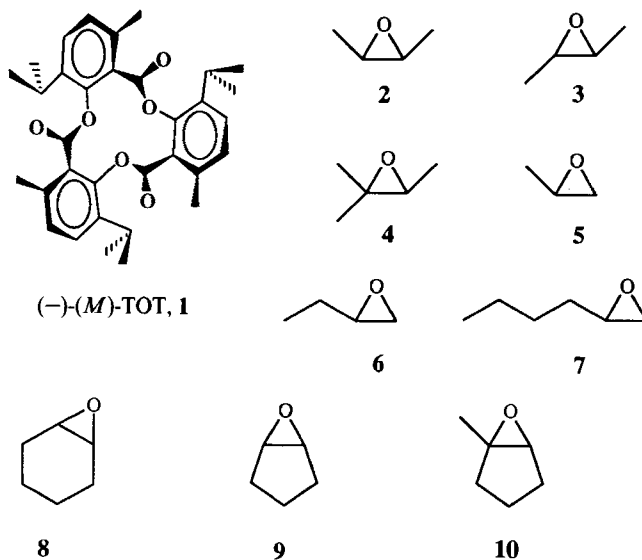


Fig. 1. Stereoview (along the  $c$  axis) of the *TOT* molecules ( $M$  configuration) bordering the cage of a clathrate belonging to the space group  $P3_121$ . For clarity, the top molecule was removed. The crystallographic  $a$  and  $b$  axes are shown. The crystallographic twofold axis, passing through the cavity, lies parallel with the vertical  $b$  axis.

cage onto its prochiral substrate [2]. With the purpose of gaining further control over the use of bulkier and more accessible external reactants, hydrogen halides were chosen as potential candidates. Attention was focused on oxirane derivatives as suitable substrates (see **2–10**) because of their high reactivity and the fairly large number of different substitution patterns fitting the cage dimensions. It is shown here that, depending on the structure, the chemical behavior of oxiranes is greatly and specifically modified by the host environment with respect to their reactivity in solution.



**2. The Action of HCl and HBr on Enclathrated Oxiranes.** – TOT was not affected by gaseous or aqueous HCl or HBr ( $\text{HX}_g$  and  $\text{HX}_{aq}$ , resp.), even not after long exposure at higher temperatures. HI failed to induce any reaction on included guests, probably owing to its molecular volume that increases the barrier to diffusion within the host lattice to prohibitive values. The occurrence of the reactions *within the cages* was supported by two observations: firstly, the reacted clathrate crystals had to be heated *in vacuo* (160–180°) to release the product(s), and secondly, X-ray powder diagrams showed that the host lattice was preserved during the reaction. It was only after complete and vigorous desolvation that the transition to the orthorhombic phase of unsolvated TOT was observed. This is an important difference with respect to the zeolitic inclusion compounds, the framework of which generally remains stable after subsequent removal of the guest. A further specific difference lies in the framework topology of the zeolitic or other microporous catalysts where the cavities are mutually interconnected through an array of tunnels reaching the crystal surface [3]. In TOT clathrates of the cage type, the external reactant has to migrate through host molecule aggregates to gain access to the isolated reaction sites.

Depending on the nature of the observations aimed at, the reactions were carried out either on microcrystalline clathrate conglomerates or on optically pure crops ( $ee > 95\%$ ) obtained by seeding with microcrystals of one antipode a TOT solution in the guest. Heterogeneous solid-gas and solid-liquid systems were investigated. In the first one, microcrystals were reacted in a gas flow of anhydrous hydrogen halide; in the second, a suspension of microcrystals was gently stirred in an aqueous solution of hydrogen halide. End products were essentially the same in both systems, nevertheless some characteristics of the transformations (rates, yields, *etc.*) were influenced by the state of the external phase. Prochiral and chiral substrates were reacted; in the latter case it is born in mind that, in a single crystal, diastereoisomeric paths are run concurrently owing to the distinct distributions of the guest enantiomers among homochiral cages. This occurrence was later shown to be of little importance for the interpretation of the results. The epoxide functionality is very sensitive to the action of strong acids. The majority of hydrogen-

Scheme 1

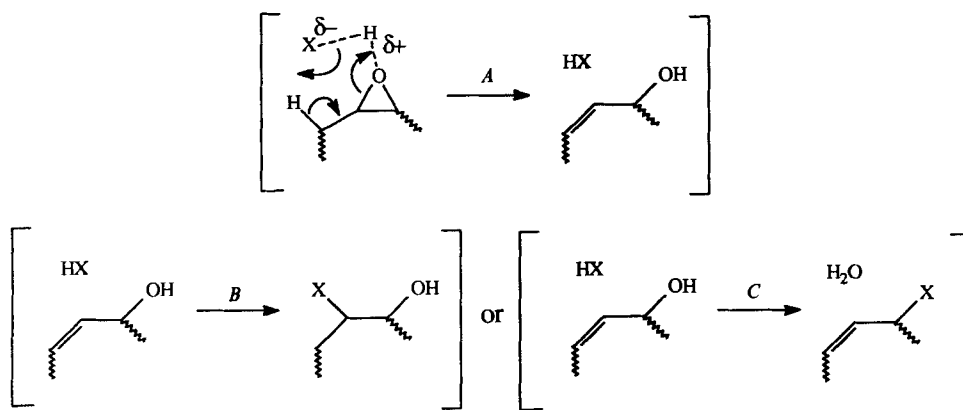


Table 1. General Chemical Behavior of Oxiranes as Guests in TOT Clathrates<sup>a)</sup>

| Oxirane         | Reactant (gaseous) | Temp., time     | Product(s) <sup>b)</sup>     | Yield [%]     |
|-----------------|--------------------|-----------------|------------------------------|---------------|
| 2               | HX <sup>c)</sup>   | <i>Scheme 2</i> | but-3-en-2-ol                | 100           |
| 3               | HX <sup>c)</sup>   | <i>Scheme 2</i> | 3-halobutan-2-ol             | 100           |
| 4               | HX <sup>c)</sup>   | <i>Scheme 2</i> | 3-halo-3-methylbutan-2-ol    | 100           |
| 5               | HCl                | 70°, 6 h        | prop-2-en-1-ol               | 90            |
|                 |                    |                 | 1-chloropropan-2-ol          | 6             |
|                 |                    |                 | 2-chloropropan-1-ol          | 4             |
| 5               | HBr                | 22°, 0.5 h      | prop-2-en-1-ol               | 64            |
|                 |                    |                 | 3-bromoprop-1-ene            | 16            |
|                 |                    |                 | 1-bromopropan-2-ol           | 11            |
|                 |                    |                 | 2-bromopropan-1-ol           | 9             |
| 6               | HBr                | 22°, 1 h        | <i>cis</i> -but-2-en-1-ol    | 36            |
|                 |                    |                 | <i>cis</i> -1-bromobut-2-ene | 12            |
|                 |                    |                 | 2-bromobut-1-ene             | 16            |
|                 |                    |                 | 2-bromobutan-1-ol            | 21            |
|                 |                    |                 | 1-bromobutan-2-ol            | 15            |
| 7 <sup>d)</sup> | HBr                | 22°, 1 h        | 2-bromohexan-1-ol            | 50            |
|                 |                    |                 | 1-bromohexan-2-ol            | 50            |
| 8               | HCl                | 70°, 6 h        | 3-chlorocyclohex-1-ene       | 94            |
|                 |                    |                 | 2-chlorocyclohexan-1-ol      | <i>ca.</i> 4  |
| 8               | HBr                | 30°, 1.3 h      | 3-bromocyclohex-1-ene        | 88            |
|                 |                    |                 | 2-bromocyclohexan-1-ol       | <i>ca.</i> 10 |

a) Space group *P*3<sub>1</sub>21.

b) The configuration of the product(s) of the relevant reactions are specified in the text.

c) HCl and HBr display the same overall action.

d) Clathrate of the channel type, space group *P*6<sub>1</sub> or *P*6<sub>2</sub>.

halide reactions with simple oxiranes were investigated in solution and involve the opening of the ring to produce two possible isomeric halohydrins [4]. Advantage of this strong affinity was already used for the detection of HCl in the ppm range after formation of derivatives and subsequent GLC [5]. The reaction control by the cage induced a striking departure from the chemical behavior in the homogeneous phase as depicted in *Scheme 1* (for convenience, enclosed guest molecules are depicted within square brackets).

As we recently showed [6], the first reaction step consists of the catalytic isomerization of the oxiranes to allylic alcohols (*Scheme 1, Step A*). Depending on the substrate, either one of two paths were then observed: addition of the hydrogen halide to the double bond to form a halohydrin (*Step B*) or nucleophilic substitution of the OH group leading to an  $\alpha\beta$ -unsaturated halide (*Step C*). By way of contrast, in solution, strongly basic reagents [7], Lewis acids [8], or vitamin B<sub>12</sub> in catalytic amounts [9] led to allylic alcohols. Isomerization by heterogeneous catalysis with solid acids or bases also proved to be practicable [10]. Most of these reactions were impaired by the presence of significant amounts of by-products. On a preliminary basis, using the stereochemical model proposed for the ring opening [11], we assumed that the cationoid end of the incoming  $H^{\delta+} \cdots X^{\delta-}$  ion pair is linked to the oxirane O-atom [12], whereas the counter ion  $X^-$  acts as a strong base capable of abstracting a proton from a  $C(\beta)$  atom. The enhanced basicity is presumably attributable to the cage environment that prohibits any conflicting solvation effect, the cage 'walls' being essentially lined with H-atoms. It is seen from *Table 1* that, if  $Br^-$

behaved as a stronger nucleophile than  $\text{Cl}^-$ , as expected, the reaction selectivity was decreased for the guests **5** and **8**. The result of the action of  $\text{HBr}_g$  on TOT/**8** deserves particular attention<sup>3)</sup>. No clathrate could be grown with the products 3-bromocyclohex-1-ene or 2-bromocyclohexanol, which means that their molecular volume exceeds that of the largest possible cage size before dislocation of the host lattice. Therefore, the reaction might occur in the absence of any ordered host environment, and deductions from results of this kind must be made with caution. The situation differs with  $\text{HCl}_g$  and TOT/**8**, because the product 3-chlorocyclohex-1-ene could be spontaneously enclathrated on recrystallization with TOT. The favorable host-guest complementarity was reflected in a considerable increase in the reaction regioselectivity.

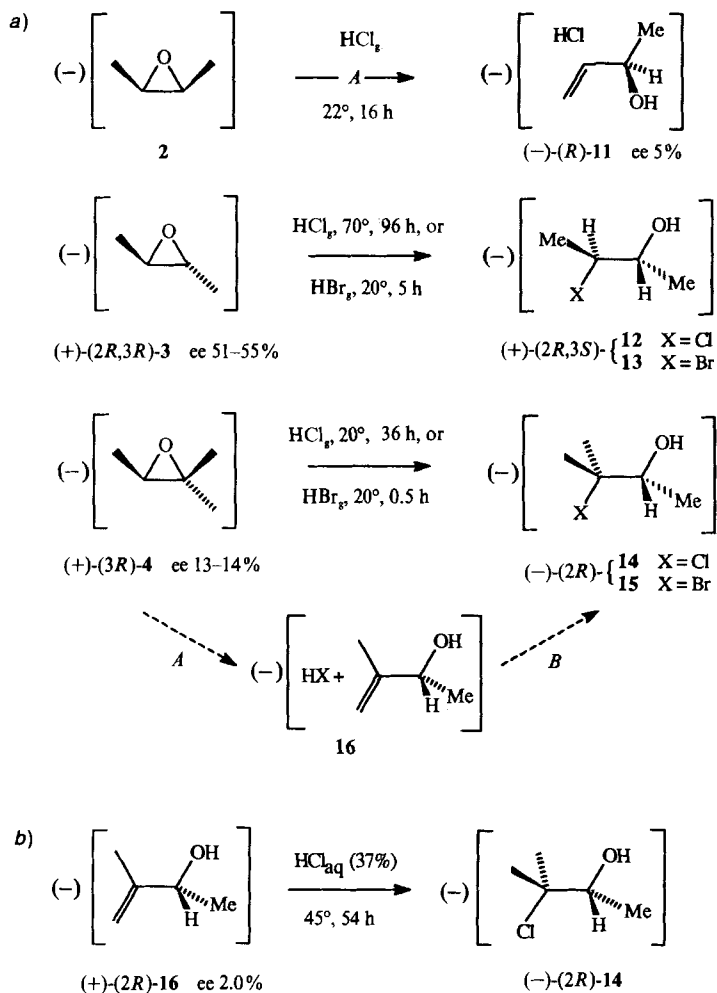
The allylic isomerization of **6** was subjected to an interesting steric control by the cage excluding the formation of a *trans*-configuration. The cage dimensions (greatest width *ca.* 7 Å) prohibit the accommodation of **6** in its extended stable conformation with a length of *ca.* 7.6 Å and force the guest into a *skew* conformation after rotation about the C(ring)–C(ethyl) bond. This was evidenced as follows: with close contacts of the non-bonded distances being monitored, fitting of **6** on the enclosed conformation of **8** [13] forces the C–C–C torsion angle to adopt a value of 64°, together with a decrease of the greatest axial length to 7.0 Å (greatest value for **8**: 7.18 Å). The bromoalkene isomers result from the action of the  $\text{Br}^-$  on the apparently 'long-lived' allylic cation surviving the C–OH<sub>2</sub><sup>+</sup> bond cleavage. The presence of 1-bromobutan-2-ol does not originate in the addition of *Step C* (Scheme 1), but might arise from a concomitant ring-opening as observed in solution, thus decreasing the selectivity of the overall transformation. No search for optimal reaction conditions were carried out for this clathrate. Enclathrated **7** underwent a ring opening similar to that expected in solution. It is pointed out that the TOT/**7** clathrate belongs to the channel-type, space group  $P6_1$ , with cell dimensions:  $a, b = 14.23$ ,  $c = 28.8$  Å. In view of earlier work [14], the guest molecules are expected to be highly disordered within channels because the length of a chain-like guest such as **7** is not supposed to fit the unit translation of the host lattice. One can conclude that specific host-guest interactions will be severely impaired or even totally absent in TOT/**7**.

The course of the reaction of TOT/**5** was sensitive to the nature of the halogen atom. No nucleophilic substitution (*Step B*) was detected from the interaction with  $\text{HCl}_g$  under the conditions given in Table 1. For increased time periods, desolvation became apparent with concomitant formation of higher amounts of chlorohydrins. Therefore, it is difficult to conclude that the formation of the chlorohydrins was exclusively taking place in the cage as might be inferred from Table 1. The overall reaction rate with  $\text{HBr}_g$  was much greater and the substitution of the OH group occurred, which might lead, for a longer reaction time, to the total disappearance of the alcohol to the benefit of allyl bromide.

**3. Stereospecific Reactions of Methyl-Substituted Oxiranes.** – The conversion of included polymethyloxiranes **2–4** proceeded through stereospecific mechanisms on treatment with anhydrous hydrogen halides in solid-gas systems. The complete transformation to the final halohydrins in 100% yield was achieved under the conditions reported in Scheme 2, a).

<sup>3)</sup> Several experiments under varied conditions were carried out, displaying apparently 'erratic' molecular ratios of the products.

Scheme 2



The conversion of **2** was limited to the catalytic isomerization to but-3-en-2-ol; no chloro compound could be detected (by NMR) for any reasonable length of reaction time (see above, reactivity of **5**). The absolute configuration of but-3-en-2-ol (**11**) being known [15], the asymmetric induction in the rearrangement of **2** was calculated on the basis of the residual optical activity measured after the racemization of the TOT of a clathrate antipode. A small ee of 5% was determined, that might be correlated with the low spontaneous enantioselectivity of TOT for **11**. To test the electrophilic properties of enclathrated but-3-en-2-ol, the TOT/**11** clathrate was grown separately and reacted for 72 h at 24° without noticeable change in the guest, thus corroborating the above observation. The contact of anhydrous HCl<sub>g</sub> with liquid **11** generated, within 2 h at -10°, a

mixture of unreacted **11** (20%), 3-chlorobut-1-ene (18%), *trans*-but-2-en-1-ol (*ca.* 30%), and *trans*-1-chlorobut-2-ene (*ca.* 30%). Stereospecific hydrohalogenation of chiral **3** and **4** allowed the determination of the absolute configuration of the four corresponding halohydrins **12–15** [16] using to advantage the previously known configurations of the substrates [17] for the assessment of their ee in the clathrates by complexation GLC [18] after desolvation (*Table 2*). An in-depth study of the reactivity of TOT/**3** under various conditions did not reveal the expected allylic intermediate (*Step A*). In accordance with the other reactions investigated, it is believed that, in this case, the allylic isomerization might be rate-determining in a two-step reaction. Interestingly, no chlorohydrin was formed on reacting liquid but-3-en-2-ol with anhydrous HCl<sub>g</sub>. In contrast with **3**, the concentration variations of the intermediate allylic alcohol **16** derived from **4** within the cage could be established and used in kinetic calculations (see below). With a view to compare the chemical behavior in the crystalline state with that in the liquid phase, anhydrous HX<sub>g</sub> was bubbled through pure trimethyloxirane (**4**) for 1 h at 0°, yielding in each case a mixture of products, *i.e.* with HCl<sub>g</sub> 3-chloro-3-methylbutan-2-ol (63%), 3-chloro-2-methylbutan-2-ol (36%), and 3-methylbutan-2-one (traces), and with HBr<sub>g</sub> 3-bromo-3-methylbutan-2-ol (43%), 3-bromo-2-methylbutan-2-ol (27%), 3-methylbutan-2-one (8%), and 2,3-dibromo-2-methylbutane (22%). It will be noted that under these particular conditions, the attacking nucleophile was introduced predominantly at the most substituted C-atom.

The observation of the intermediate 3-methylbut-3-en-2-ol (**16**) suggested the opening of an alternative route to **14** *via* the clathrate TOT/**16** grown separately. This clathrate was easily accessible either as conglomerates of microcrystals or as batches of seeded microcrystals of high optical purity (> 95%). Addition of 1 equiv. of HCl could be accomplished quantitatively at 22° within 36 h in the solid-gas system. These reaction conditions were very similar to those necessary to convert the parent oxirane **4**. The reaction was somewhat more sluggish with HCl<sub>aq</sub> necessitating 54 h at 45° for the quantitative conversion of **16** to **14**. On flash desolvation of the reacted clathrate at 180°,

Table 2. Absolute Configuration of Halohydrins Formed by Stereospecific Hydrohalogenation of Enclathrated Oxiranes [16]

| Substrate <sup>a)</sup>  | Products   | Optical rotation   |
|--|--|--|
| (+)-(2 <i>R</i> ,3 <i>R</i> )-2,3-Dimethyloxirane ( <b>3</b> ) | (+)-(2 <i>R</i> ,3 <i>S</i> )-3-chlorobutan-2-ol ( <b>12</b> ) | $[\alpha]_D^{25} = +9.1$ ( $c = 9$ , CHCl <sub>3</sub> ), $+9.3^b$ (neat)  |
|  | (+)-(2 <i>R</i> ,3 <i>S</i> )-3-bromobutan-2-ol ( <b>13</b> )  | $[\alpha]_D^{20} = +18.3$ ( $c = 10$ , CHCl <sub>3</sub> )                 |
| (+)-(3 <i>R</i> )-2,2,3-Trimethyloxirane ( <b>4</b> )          | (-)-(2 <i>R</i> )-3-chloro-3-methylbutan-2-ol ( <b>14</b> )    | $[\alpha]_D^{20} = -3.1^d$ ( $c = 9$ , CHCl <sub>2</sub> ), $-3.1$ (neat)  |
|  | (-)-(2 <i>R</i> )-3-bromo-3-methylbutan-2-ol ( <b>15</b> )     | $[\alpha]_D^{20} = -5.6$ ( $c = 23$ , CHCl <sub>3</sub> ), $-6.1^e$ (neat) |

<sup>a)</sup> Major enantiomer in (-)-(*M*)TOT.

<sup>b)</sup> In good agreement with the reported  $[\alpha]_D = +9.77$  [19].

<sup>c)</sup> Complementary value measured from (+)-TOT:  $[\alpha]_D = -17.7$  ( $c = 14$ , CHCl<sub>3</sub>).

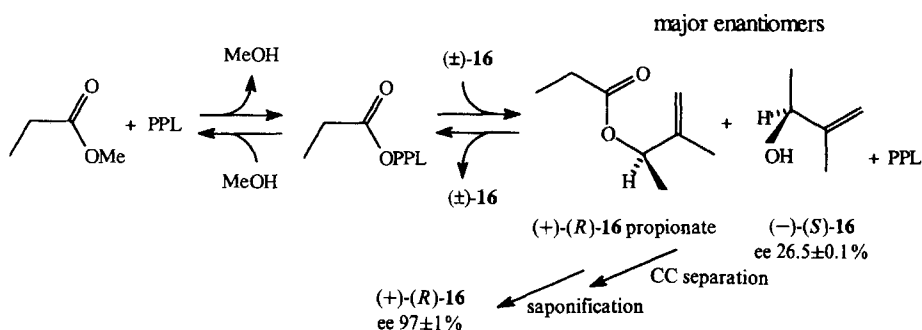
<sup>d)</sup> Complementary value:  $[\alpha]_D = +3.1$  ( $c = 16$ , CHCl<sub>2</sub>); see revised values for (2*R*)- and (2*S*)-**14** obtained from the hydrohalogenation of enclathrated 3-methylbut-3-en-2-ol (**16**) (*Table 3*).

<sup>e)</sup> Complementary value:  $[\alpha]_D = +5.8$  (neat).

a constant amount of *ca.* 10% of **14** was thermally dehydrohalogenated to produce 3-methylbutan-2-one, in conformity with earlier observations [20].

The knowledge of the *ee* in TOT/**16** is a prerequisite to the determination of the configurational properties of product **14**. The enantiomer (+)-**16** was shown to have the (*R*)-configuration, with  $[\alpha]_D = +5.6 \pm 1$  [21]. The large reported standard error entails considerable uncertainties in the configurational parameters we purposed to specify; therefore, we turned to establishing the absolute configuration of **16** with higher accuracy. The application of enzymes as chiral catalysts to the preparation of chiral compounds has attracted greater attention during the last few years. The enzyme-catalyzed asymmetric transesterification of chiral alcohols by the porcine pancreatic lipase (PPL) was used to resolve series of secondary alcohols with high enantiomeric purity [22]. This methodology lent itself efficiently to the resolution of **16**. The kinetic selectivity afforded a high excess of propionate derived from (+)-(*R*)-**16**, besides a predominant amount of unchanged (–)-(*S*)-**16** (Scheme 3). After CC separation and saponification, the enantiomeric purity of both fractions was asserted on examination of the <sup>1</sup>H-NMR and <sup>19</sup>F-NMR spectra of the diastereoisomeric esters derived from (+)-(*R*)- $\alpha$ -methoxy- $\alpha$ -(trifluoromethyl)phenylacetic acid [23] (= 3,3,3-trifluoro-2-methoxy-2-phenylpropionic acid = MTPA). Subsequent polarimetric measurements of the enantiomeric **16** gave access to improved values for the specific rotation  $[\alpha]_D^{20}$  as reported in Table 3.

Scheme 3

Table 3. Revised Specific Rotation of 3-Methylbut-3-en-2-ol (**16**) and 3-Chloro-3-methylbutan-2-ol (**14**)<sup>a</sup>

|                                       | $[\alpha]_D^{20}$ (neat) | $[\alpha]_D^{20}$ (CHCl <sub>3</sub> ) |                                       | $[\alpha]_D^{20}$ (neat) | $[\alpha]_D^{20}$ (CHCl <sub>3</sub> ) |
|---------------------------------------|--------------------------|--|---------------------------------------|--------------------------|--|
| (2 <i>R</i> )- <b>16</b> <sup>b</sup> | +5.64 ± 0.18°            | +5.76°                                 | (2 <i>R</i> )- <b>14</b> <sup>d</sup> | –3.70 ± 0.17°            | –3.61 ± 0.20°                          |
| (2 <i>S</i> )- <b>16</b>              | –5.35 ± 0.09°            | –5.78°                                 | (2 <i>S</i> )- <b>14</b>              | +3.57 ± 0.18°            | +3.61 ± 0.20°                          |
| mean $[\alpha]_D^{20}$                | (±)5.50 ± 0.21°          | (±)5.77 ± 0.06° <sup>c</sup>           | mean $[\alpha]_D^{20}$                | (±)3.64 ± 0.28°          | (±)3.61 ± 0.20° <sup>e</sup>           |

<sup>a</sup>) Standard errors at the 0.05 significance level.

<sup>b</sup>) Kinetically selected (Scheme 3).

<sup>c</sup>) Concentration *c* = 8.

<sup>d</sup>) From (–)-TOT/(+)-(2*R*)-**16**.

<sup>e</sup>) Averaged over concentrations varying from *c* = 8 to 29.



The enantioselectivity of the TOT/**16** clathrate was established by way of desolvated samples of the guest from complementary antipodes of the clathrate. The ee in each sample was measured by two different methods, *i.e.* by the MTPA methodology described above and by chiroptical measurements including the specific rotation of **16**. Thus, the ee for (–)-TOT/**16** was  $1.96 \pm 0.08\%$  (MTPA) and  $2.04 \pm 0.02\%$  (polarimetry) and for (+)-TOT/**16**  $1.96 \pm 0.08\%$  (MTPA) and  $2.07 \pm 0.02\%$  (polarimetry). The enantioselectivity appears exceptionally low but is nevertheless significantly ascertained: the average value  $2.01 \pm 0.06\%$  was subsequently used in the calculation of the specific rotation of **14**. The hydrochlorination of **16** was carried out according to *Scheme 2, b*. The configuration of the asymmetric C-atom was not modified by the addition to the double bond, hence the ee of **14** in the cage could be safely assumed to be equal to that of the substrate **16**. Polarimetric measurements on the recovered product are reported in *Table 3*.

By way of comparison, the chemical reactivity of **16** in the homogeneous phase was revealing. The action of  $\text{HCl}_{\text{aq}}$  (37%; 3 h, 45°) led to a complex mixture consisting of 3-methylbutan-2-one (65%), 3-chloro-2-methylbut-1-ene (10%), 2,3-dichloro-2-methylbutane (20%), and unidentified by-products (5%), with no halohydrin being detected. As was usually observed, the action of anhydrous  $\text{HCl}_{\text{g}}$  was more specific: a mixture of **14** (89%) and 3-methylbutan-2-one (11%) was produced within 3 h at 22°. It is reminded that neither  $\text{HCl}_{\text{g}}$  nor  $\text{HCl}_{\text{aq}}$  induced the formation of a ketone within the clathrate.

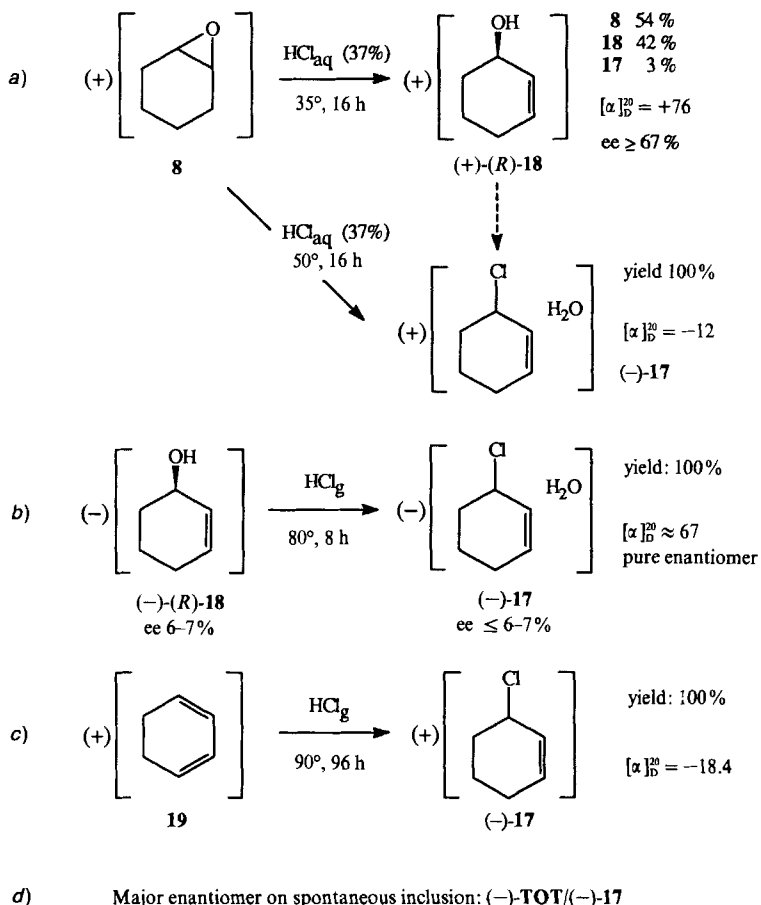
#### 4. On the Determination of the Absolute Configuration of 3-Chlorocyclohex-1-ene. –

The 3-chlorocyclohex-1-ene (**17**) was obtained from three different substrates without the formation of interfering by-products (*Scheme 4*). The two reactions involving the prochiral substrates **8** and cyclohexadiene (**19**) demonstrated the occurrence of chirality transfer from the cage onto the product. The most representative reaction was the two-step conversion of **8** by cage-specific allylic isomerization to cyclohex-2-en-1-ol **18** followed by the nucleophilic substitution of OH by Cl (*Step C*) to furnish **17** in 100% yield (by  $^1\text{H-NMR}$ ; *Scheme 4, a*). When the reaction was stopped under well established conditions, a salient feature emerged, *i.e.* the high ee of the intermediate **18**. This feature, in conjunction with the phenomenon of chirality amplification, was subsequently used in the enantiomeric enrichment of 3-chlorocyclohex-1-ene. Reports are available on the resolution of **18** establishing the (+)-(*R*)-configuration [24], which was the one preferentially included in (–)-TOT. The reported  $[\alpha]_{\text{D}}^{20} = +112$  [24] was used for the determination of the enantioselectivity of the TOT/**18** clathrate to give magnitudes of 6.0 and 6.5% from the (+)- and the (–)-TOT antipodes, respectively, with an estimated standard error of  $\pm 0.5\%$  for each single measurement<sup>4</sup>). In clathrate batches of high enantiomeric purity, **18** underwent a complete conversion to deliver chemically pure **17** showing an important optical activity. Considering the ee's above and postulating a clean inversion of configuration in the process, a provisory specific rotation of **17** is accessible at the present stage of our research, with the average value  $[\alpha]_{\text{D}}^{20} = -67 \pm 4$  (see *Scheme 4, b*).

Another convincing evidence of chirality transfer was found in the conversion of **19** to **17**. Due to the relatively slow rate in the solid-liquid system, the reaction was carried out

<sup>4</sup>) The heterogeneous nature of the unknown inclusion mechanism induced, within limits, random fluctuations in the actual ee from one sample to the other.

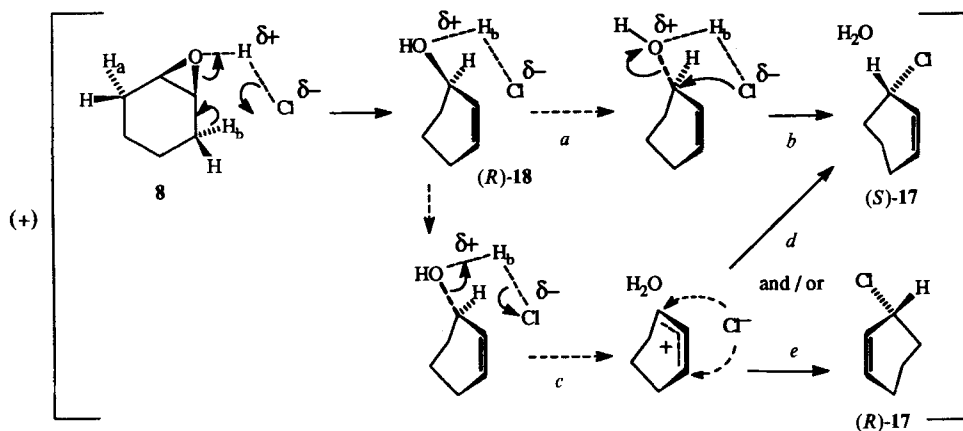
Scheme 4



between anhydrous  $\text{HCl}_g$  and both TOT/19 antipodes to produce, in each case, a chemically 100% pure product showing optical rotations of  $-18.4$  and  $+17.6$ , respectively. Sign correlations and optical activities are reported in *Scheme 4* for each reaction. Both complementary pathways were studied, but the depicted ones were selected so as to end up in the predominant formation of levorotatory 17; so it became clear that, as end-product, 17 could be found in either one of the cage antipodes depending on the substrate. In addition, it is emphasized that (-)-TOT exhibited a higher discrimination for (-)-17 in the process of spontaneous inclusion. This feature compared well with the optical rotation of 17 measured in each reaction: when generated in the (-)-TOT lattice, (-)-17 had a higher  $[\alpha]_D$  (*i.e.* a higher *ee*) than when it was formed in the cage of opposite chirality where the host-guest complementary is much less favorable. It is, however, pointed out that the allylic isomerization of 8 gave rise to a high *ee* of the alcohol in an environment of opposite chirality to that observed on spontaneous inclusion (about an order of magni-

tude less). Indeed, this is a puzzling result and, unfortunately, no structural information is at hand at present to allow a packing-energy calculation of the crystalline diastereoisomer generated from TOT/8. It is further noted that the nucleophilic attack on **18** in the second step (see *Scheme 4a*) must necessarily proceed with considerable retention considering the low  $[\alpha]_D$  of **17** compared with that shown in the one-step process (see *Scheme 4b*). Finally, a brief survey of the possible reaction mechanisms leading from **8** to **17** is displayed in *Scheme 5*. Within the cage, a bimolecular reaction can be safely assumed between **8** and the incoming  $H^{\delta+}Cl^{\delta-}$  ion pair, with the initial protonation of the O-atom to form an intermolecular 'oxonium complex' as usually suggested for the ring opening in acidic media [4]. As supporting evidence, the formation of an [oxirane  $\cdots HCl$ ] complex was recently observed in the gas phase [25]. On the basis of the stereochemical model proposed for *E2 trans*-elimination, the diastereotopic protons  $H_a$  and  $H_b$  are the most likely to be abstracted by  $Cl^-$  owing to the strongly enhanced basic character of the latter in the cage. Experimental results disclose that the (+)-cage environment favors the elimination of  $H_b$ , that will then be easily translated without much steric hindrance to be linked to the OH group. Leaving out host-guest interactions, either one of two limiting cases can be envisaged as subsequent reaction step: the heterolytic dissociation of **18** to an allylic carbocation (*Path c*) or a direct displacement of OH without intermediate, involving a clean inversion of configuration (*Path a* and *b*). The issue of the carbocation reaction is twofold depending on the site of attack by  $Cl^-$  and on the reasonable assumption that the confines of the cage prevents the nucleophile from 'jumping' from one side of the ring to the other. Attack at one end of the delocalized carbocation corresponds to an inversion (*Path d*), whereas attack at the other end requires retention (*Path e*). In terms of the 'topochemical principle' [26], which states that reaction in solids will take place with a minimum of molecular (or atomic) motion, we assume that  $S_N2$  substitution (*Path a* and *b*) might be favored, because the Cl-atom, as anionic part of the  $H^{\delta+}Cl^{\delta-}$  ion pair, is bound to be sterically close to the C-atom linked to the OH group after formation of **18**. In the case of the carbocation being present, the same stereochemical implications are also favorable for attack on the C-atom formerly bonded to OH, with the additional

Scheme 5



support of the generally fast combination of highly electrophilic carbocations with vicinal *Lewis* bases. Combined chemical, crystallographic, and molecular-modelling calculations are presently being applied to a more evidential elucidation of the reaction mechanisms and to the absolute configuration of **17**.

The chemical reactivity of the guests **9** and **10**, which are structurally related to **8**, was studied under the action of  $\text{HCl}_{\text{aq}}$  (36%). Surprisingly, **9** was relatively inactive below 60°. Above this temperature and over a period of 72 h, the reaction was complete and gave 3-chlorocyclopent-1-ene (44%) and 2-chlorocyclopentan-1-ol (44%), mixed with unidentified products. The methylated derivatives **10** demonstrated a somewhat higher reactivity from 40° upwards. The reaction mixture sampled over a period of 22 h showed the formation of 2-chloro-1-methylcyclopentan-1-ol and 3-chloro-2-methylcyclopent-1-ene in a constant 2:1 molecular ratio. The presence of 3-chlorocyclopent-1-ene (from **9**) and 3-chloro-2-methylcyclopent-1-ene (from **10**), as homologues of **17** (from **8**) suggests the occurrence of the typical allylic isomerization as the first reaction step; however, the OH functionality could not be detected in either of the reaction mixtures. For lack of specificity, these reactions were not further investigated.

**5. Kinetic Measurements.** – The knowledge of the concentration variations of the substrate and product(s) may allow one to make some choice among plausible mechanisms within the cage. Thus, the time-dependent molecular ratios of the reactants in batches of reacted clathrate were determined by peak integration of  $^1\text{H-NMR}$  spectra and expressed as dimensionless relative concentrations in the calculations. Quantitative results of relevant reactions are reported in *Table 4* and depicted in *Figs. 2* and *3*. The bimolecularity of the reactions is well established in view of the confinement of the reactants in the cage. The major stumbling block in the interpretation of solid-state kinetic data in terms of rate expressions for liquid solutions is the phenomenological and mathematical description of the anisotropic mass transport in the crystal. In a recent comprehensive study of the molecular packing of TOT cage clathrates, two small entry channels leading into the cavity were detected [27], which are symmetry-equivalent and situated at either end of the longest axial dimension of the cage (*ca.* 7 Å) which is perpendicular to the twofold crystallographic axis. The cross-section at the bottleneck of the entry channel, measured using the TOT/2-bromobutane coordinates and considering *van der Waals* radii, is 'peanut shell' shaped, *ca.* 3.6 Å in height and 1.25 Å in width. These small interlacing channels control certainly to a large extent the diffusion path of the migrating reactant. The presence of cage vacancies<sup>5)</sup> confers an additional degree of motional freedom to the migrating  $\text{H}^{\delta+}\text{Cl}^{\delta-}$  reactant. The phenomenon of defect mobility must also be taken into account. Diffusion along dislocations are bound to decrease the reaction selectivity, when the bordering cages are affected. A consistent model for the volume diffusion of an external molecular agent into a molecular crystal is lacking for the present, although calculations of the diffusivities of reactants in zeolitic catalysts were performed [28]. As a consequence, heterogeneous kinetic data for **2–4** were tentatively rationalized in terms of the rate expressions applied to liquid solutions. Interestingly, striking similarities were disclosed. The reactions were carried out in  $\text{HCl}_{\text{aq}}$  of known concentrations and at fixed temperatures to maintain the reaction times within limits

<sup>5)</sup> Cage vacancies are an intrinsic property of TOT cage clathrates. Guest occupancy factors from 0.6 to 0.8 are commonly encountered, depending on the guest structure and/or the conditions of growth.

Table 4. Rates and Experimental Orders for Some TOT Clathrate Reactions

| Substrate | [HCl] <sup>a)</sup> | Temp. [°C] | <i>k</i>            | <i>n</i> <sup>b)</sup> | Σ err <sup>2c)</sup> |
|-----------|---------------------|------------|---------------------|------------------------|----------------------|
| <b>2</b>  | 11.6                | 40         | 0.168 <sup>d)</sup> | 1                      | 0.010 <sup>e)</sup>  |
|           |                     |            | 0.168 <sup>f)</sup> | 1 <sup>f)</sup>        | 0.028                |
|           |                     |            | 0.143               | 1 <sup>f)</sup>        | 0.011 <sup>g)</sup>  |
|           |                     |            | 0.122               | 0.7                    | 0.005 <sup>g)</sup>  |
| <b>3</b>  | 11.58               | 60         | 0.058 <sup>d)</sup> | 1                      | 0.007 <sup>e)</sup>  |
|           |                     |            | 0.058 <sup>f)</sup> | 1 <sup>f)</sup>        | 0.144                |
|           |                     |            | 0.144               | 2 <sup>f)</sup>        | 0.012 <sup>g)</sup>  |
|           |                     |            | 0.167               | 2.3                    | 0.011 <sup>g)</sup>  |

| Substrate <sup>h)</sup> | [HCl] <sup>a)</sup> | Temp. [°C] | <i>k</i> <sub>1</sub> <sup>i)</sup> | Σ err <sup>2</sup> | <i>k</i> <sub>2</sub> <sup>i)</sup> | Σ err <sup>2</sup> |
|-------------------------|---------------------|------------|-------------------------------------|--------------------|-------------------------------------|--------------------|
| <b>4</b>                | 10.97               | 22         | 0.870                               | 0.005              | 0.032                               | 0.012              |
|                         | 9.10                | 22         | 0.116                               | 0.005              | 0.0035                              | 0.0012             |
|                         | 7.94                | 22         | 0.034                               | 0.002              | 0.000 <sup>j)</sup>                 | –                  |
|                         | 6.86                | 22         | 0.011                               | < 0.001            | 0.000                               | –                  |

a) Concentration of the aqueous solution in mol/l.  
b) Reaction order.  
c) Comparison between data set and calculated concentration-time profile.  
d) From the logarithm data plot.  
e) Σ err<sup>2</sup> of the logplot.  
f) Fixed as constant in the integrated rate expression.  
g) Minimized by least-squares analysis, see text.  
h) Selected values, see Fig. 3.  
i) *k*<sub>1</sub> and *k*<sub>2</sub> in h<sup>-1</sup>.  
j) Too small to be measured.

(20–30 h) preventing unwanted desolvation. The use of conglomerates prevented any distinction to be made between diastereoisomeric reaction paths, resulting in ‘average’ values for the derived kinetic parameters.

A first-order reaction rate was firstly assumed for the one-step conversion of **2** and **3**. The plot of the functions  $\ln c = -kt$ , where *c* denotes the relative concentration of the substrate at time *t*, gave linear regressions with correlation factors larger than 0.998 (see Table 4 and Figs. 2a,b). The rate constant *k* was 0.168 h<sup>-1</sup> for **2** and 0.058 h<sup>-1</sup> for **3**. It was later shown that linear logarithmic relationships may be biased with respect to the assumed first-order rate function. This was especially obvious in the kinetics of **3** (Fig. 2e), where the measured concentrations appeared systematically shifted to lower values by a roughly constant factor with respect to the calculated first-order concentration-time curve. This bias did not affect the linearity of the regression line but only the intercept that should take the value  $\ln c = 0$  for *t* = 0 (see Figs. 2a, b). A more rewarding approach to the treatment of the kinetic data of **2** and **3** was the minimization of the sum of squares of the differences between the observed *c* and the values derived from the assumed rate law. Minimization was performed by varying *k* and the reaction order *n* in the integrated form of the rate law  $dc/dt = -kc^n$ , where *n* may assume non-integer values. The first-order concentration-time profile using the above *k* = 0.168 h<sup>-1</sup> value led to an unreasonably high standard error ( $\sigma = 0.168$ ) when compared to the data set of **2**. Optimization of *k* and *n* brought about a significant improvement with *k* = 0.122 ± 0.030 and an empirical order *n* = 0.7, still in fair agreement with the allylic isomerization first order in the

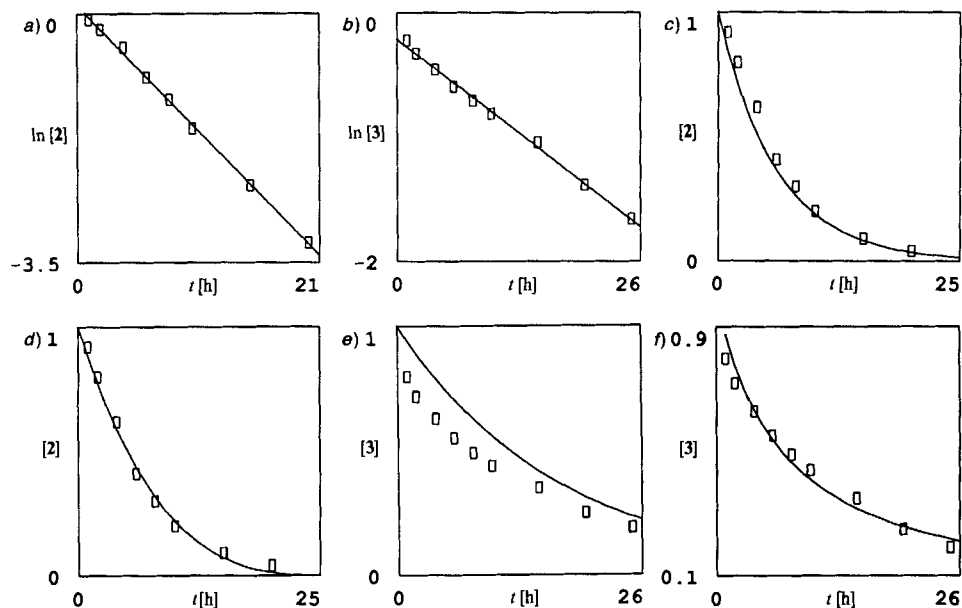


Fig. 2. Kinetic data for the reactions of **2** and **3**. a) b) Logarithm plots and c–f) measured relative concentrations vs. time ( $\square$ ) and calculated concentration-time profiles. c) e) Calculated curve using the rate constant derived from the log plot. d) f) Calculated curve using the optimized  $k$  and  $n$  values (Table 4).

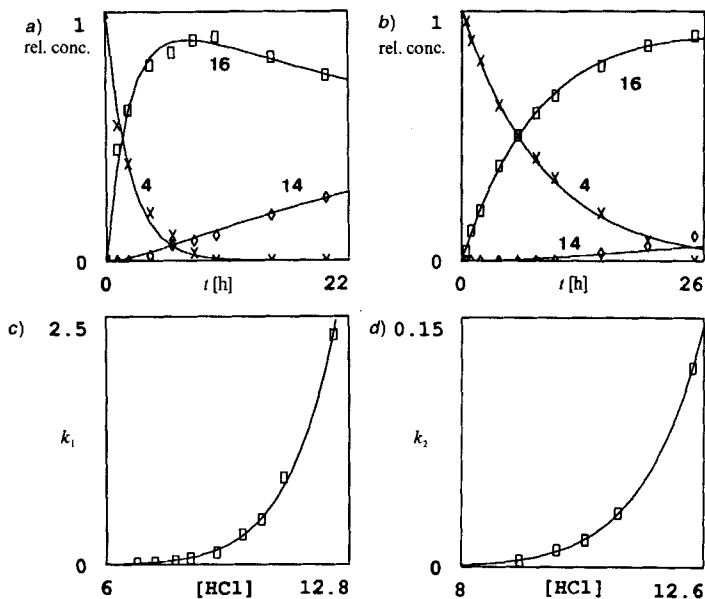


Fig. 3. a) b) Selected concentration-time profiles of the consecutive first-order reactions  $4 \rightarrow 16 \rightarrow 14$  (the integrated rate-law expressions [29] (solid curves) are fitted on the data by a least-squares procedure; concentration of  $HCl_{aq}$ , 10.35 and 9.10 mol/l, resp.;  $k_1 = 0.447$  and 0.116, and  $k_2 = 0.016$  and 0.0035, resp.). c) d) Variation of  $k_1$  and  $k_2$ , respectively, as a function of the concentration of the external reactant  $HCl_{aq}$  ( $[HCl]$  in mol/l;  $k$  in  $h^{-1}$ ).

substrate. This might reflect a fast [oxirane  $\cdots$  HCl] complex formation (entropy decrease), followed by a rate-determining molecular rearrangement (entropy increase) the 'concentration' (molecularity) of HCl remaining constant in the cage during the processes<sup>6</sup>).

In contrast with **2**, the conversion of **3** showed an optimized reaction order of  $n = 2.3$  (Fig. 2f) that expresses the participation of HCl in a second-order reaction rate, the cage environment promoting the necessary 1:1 stoichiometric ratio of the reactants<sup>7</sup>). The apparent departure from an ideal second-order mechanism cannot be attributed to experimental errors, but reflects the inadequacy of the rate law used, when applied to the solid state. It is not possible, at this stage, to decide experimentally which of two mechanistic alternatives is occurring: the ring-opening addition of HCl with formation of halohydrin, or the rate-determining formation of an intermediate allylic alcohol preceding the fast HCl addition to the olefinic bond.

The intermediate occurrence of 3-methylbut-3-en-2-ol (**16**) was observed in the reaction of **4** and the concentration-time data measured. The overall kinetics agreed well with a process involving two successive first-order (or pseudo-first-order) steps, such as **4**  $\rightarrow$  **16** ( $k_1$ ) and **16**  $\rightarrow$  **14** ( $k_2$ ; Figs. 3a, b). A number of possible mechanisms are suggested in Scheme 5 by analogy with the chemical behavior of **8**. The rates  $k_1$  and  $k_2$  were calculated on the basis of data recorded at known constant concentrations of  $\text{HCl}_{\text{aq}}$  and are expressed in  $\text{h}^{-1}$ . By this is meant that the rate expressions refer to interactions arising within the limits of the crystal lattice. Thus, a slight change in the  $\text{HCl}_{\text{aq}}$  concentration induced drastic modifications of the rates of the intracrystalline reactions. It is believed that alterations in the outer diffusion layer, at the borderline clathrate-liquid, were partially responsible for these modifications. All things being equal, the average flux of HCl into the solid is supposed to be constant for a given weight of microcrystals, the size distribution of which having been shown to be reproducible owing to the standardized method of preparation. The determination of the  $k$ 's as functions of the  $\text{HCl}_{\text{aq}}$  concentration gave the empirical equations  $k_1 = (3.429 \pm 0.025) \cdot 10^{-10} \cdot [\text{HCl}]^9$  and  $k_2 = (1.146 \pm 0.001) \cdot 10^{-13} \cdot [\text{HCl}]^{11}$  where  $[\text{HCl}]$  denotes the concentration of  $\text{HCl}_{\text{aq}}$  in mol/l (Figs. 3c, d). The coefficient  $a$  and the integer exponent  $n$  were optimized by a least-squares method applied to the postulated relationship  $k = a [\text{HCl}]^n$ . By way of example, the  $k_1$  equation may be substituted for the rate constant in the first-order rate of change of **4**, giving the rate expression for the first step of the heterogeneous reaction<sup>8</sup>):  $d[\mathbf{4}]/dt = -3.43 \cdot 10^{-10} \cdot [\mathbf{4}] \cdot [\text{HCl}]^9$ , where  $[\text{HCl}]$  is maintained constant. Such a large reaction order of 9 in a reactant is unlikely to be found for reactions in liquid solutions. The major contribution to the barrier to the crossing of the liquid-solid interface by a 'naked' HCl molecule is the energy necessary for the disruption of the solvation shell surrounding the molecule in solution. This view was supported by the ratio of the first-order rate constants ( $\text{h}^{-1}$ ) of reactions of **4** carried out with anhydrous  $\text{HCl}_g$ , for which  $k_1 = 7.3$  and  $k_2 = 0.38$ , and with  $\text{HCl}_{\text{aq}}$  (38%), for which  $k_1 = 2.3$  and  $k_2 = 0.12$ . The solid-gas reaction

<sup>6</sup>) Not considering the intra-crystalline diffusion time, a minute amount of HCl may theoretically induce the isomerization of all the guests in a single crystal.

<sup>7</sup>) The integrated form used is  $c = [(n-1)kt + 1] \exp[-1/(n-1)]$ . The integrated rate expressions for the two first-order consecutive reactions of **4** are taken from [29].

<sup>8</sup>) It is reminded that the expression depends implicitly on the average size of the microcrystals, that is constant under the present experimental conditions. Therefore, the equation is only valid under such conditions.

was 3.2 times faster than the solid-liquid reaction for both steps with  $\text{HCl}_{\text{aq}}$  (38%), and 650 times faster than the first step of the reaction with  $\text{HCl}_{\text{aq}}$  (22.5%) for which  $k_2$  was too small to be measured.

**6. Concluding Remarks.** – Selectivity is an important feature expected of chemical reactions, particularly of catalyzed reactions. The term heterogeneous catalysis is, however, inappropriate to embody the action of TOT cage clathrates on the chemical behavior of guest molecules because active sites are lacking within the cages. On the other hand, it is a matter of definition whether these clathrates may be considered as guest biomimetic receptors with regard to the migrating reactant or as rigid H-lined solvation shells favoring specific reaction pathways. In accordance with both points of view, target products are regiospecifically formed and, in many cases, in 100% chemical yield. Chirality transfer from the cage onto prochiral substrates is also observed. The underlying causes of the cage-specific, cage-controlled allylic isomerization are not clearly established at present. At first sight, the causes probably originate in a strong enhancement of the basicity of the unsolvated  $\text{Cl}^-$  anion, associated with the increase of the probability (steric) factor, when the reaction site of the substrate is properly oriented with respect to the 'entry channel' where it joins the cage. It seems reasonable to assume that the reactions are stereoselective not only because of the overall cage environment, but also because of the local orientation of the substrate with respect to the symmetrically localized inlets of the reactant into the cage. Further studies are under way to elucidate additional fundamental aspects of this new type of solid-state reactivity.

We are grateful to the *Swiss National Science Foundation* for financial support.

### Experimental Part

1. *General.* TLC: *Merck silica gel 60 F<sub>254</sub>* TLC plates. Prep. column chromatography: *Merck 60 silica gel*, particle size 0.063–0.200 mm. Polarimetric measurements: *Perkin-Elmer-241* polarimeter, 1-ml and 0.35-ml microcuvettes ( $l = 1$  cm).  $^1\text{H}$ - and  $^{19}\text{F}$ -NMR Spectra: *Bruker-AMX 400*, *Bruker-WM-360*, and *Varian-XL-200* spectrometers; chemical shifts  $\delta$  in ppm rel. to  $\text{SiMe}_4$  as internal reference for  $^1\text{H}$  and to  $\text{C}_6\text{F}_6$  as external reference for  $^{19}\text{F}$ ;  $J$  in Hz; quantitative analysis (molecular ratios) of complex reaction mixtures by integration of nonoverlapping  $^1\text{H}$ -NMR peaks pertaining to the different components.

2. *Microcrystals.* The general procedures for the preparation and desolvation were previously described [6] [16]. Microcrystalline batches enriched in one TOT antipode were obtained by seeding a saturated TOT soln. in the guest (10–100 ml) with powdered clathrate single crystals (20–50 mg) of the same sign; treatment of the mixture as aforesaid. The determination of the optical activity of a microcrystalline sample (10–20 mg) was performed by extrapolating, at time = 0, the logarithm plot of the racemization curve recorded at 546 nm in  $\text{CHCl}_3$ . The optical purity was calculated with respect to the specific rotation of TOT at time = 0, which was  $[\alpha]_{346}^{20} = 88.75 \pm 0.18$  at the 95% confidence limits. This value was averaged over 28 racemization curves originating from four different clathrates, the guests of which were benzene,  $\text{CH}_2\text{Cl}_2$ , MeI, and tetrahydrofuran.

3. *Kinetic Measurements. Solid-Gas:* Microcrystalline conglomerates (batch weight, several mg to g) were put on a sintered-glass surface in a thermostated reactor through which a stream of dry gaseous hydrogen halide was passed. Aliquots were rapidly withdrawn at time intervals, washed with  $\text{H}_2\text{O}$  to neutrality, dried over NaOH pellets, and examined by NMR.

*Solid-Liquid:* Suspensions of microcrystals (50–100 mg) in aq. solns. of hydrogen halide (5–10 ml) of titrated concentration were put in tightly capped or sealed tubes in a slowly rotating apparatus immersed in a thermostatically controlled bath. Quenching and drying as described above.

4. *Materials.* Methyloxirane (4), ethyloxirane (6), butyloxirane (7), and 1,2-epoxycyclohexane (8) were commercial products purchased from *Fluka*, Switzerland, and 1,2-epoxycyclopentane (9) from *Aldrich*, Switzerland.



All products were distilled and dried over 4-Å molecular sieves. Porcine pancreatic lipase, type II (PPL), was purchased from *Sigma*, Switzerland. Trio-*o*-thymotide (**1**) was synthesized by cyclodehydration of *o*-thymotic acid with POCl<sub>3</sub> [30].

*cis*-2,3-Dimethyloxirane (**2**). From *cis*-but-2-ene via *threo*-3-bromobutan-2-ol [31], which was cyclized to **2** with KOH [32]. Colorless liquid. B.p. 59–60°. <sup>1</sup>H-NMR (360 MHz, CDCl<sub>3</sub>): 1.22 (*m*, 2 CH); 2.99 (*m*, 2 Me).

*trans*-2,3-Dimethyloxirane (**3**). As described for **2**, from *trans*-but-2-ene via erythro-3-bromobutan-2-ol. Colorless liquid. B.p. 53–4°. <sup>1</sup>H-NMR (200 MHz, CDCl<sub>3</sub>): 1.23 (*m*, 2 CH); 2.65 (*m*, 2 Me).

1,2-Epoxy-1-methylcyclopentane (**10**). A suspension of 1 mol-equiv. of 1-methylcyclopent-1-ene (*Fluka*), and 1.2 mol-equiv. of 3-ClC<sub>6</sub>H<sub>4</sub>CO<sub>3</sub>H (55%; *Fluka*), and 1.2 mol-equiv. of 0.5M NaHCO<sub>3</sub> in 700 ml of CH<sub>2</sub>Cl<sub>2</sub> was vigorously stirred for 4 h at 24° [33]. Colorless liquid. B.p. 112–114°. <sup>1</sup>H-NMR (360 MHz, CDCl<sub>3</sub>): 1.32–1.70 (*m*, 2 CH<sub>2</sub>); 1.57 (*s*, Me); 1.82–2.03 (*m*, CH<sub>2</sub>); 3.24 (*br. s*, H–C(2)).

2,2,3-Trimethyloxirane (**4**). By cyclization of 3-bromo-2-methylbutan-2-ol with KOH [34]. Colorless liquid. B.p. 78°. <sup>1</sup>H-NMR (360 MHz, CDCl<sub>3</sub>): 1.24 (*s*, Me); 1.26 (*d*, *J* = 5.5, Me); 1.29 (*s*, Me); 2.84 (*q*, *J* = 5.5, CH).

3-Methylbut-3-en-2-ol (**16**). From methacroleine (= 2-methylprop-2-enol; 85%, *Aldrich*) and 3M MeMgBr in Et<sub>2</sub>O (*Aldrich*) [34]. Colorless liquid. B.p. 110°. <sup>1</sup>H-NMR (400 MHz, CDCl<sub>3</sub>): 1.28 (*d*, *J* = 6.4, Me); 1.58 (*br. s*, OH); 1.75 (*s*, Me); 4.25 (*q*, *J* = 6.4, CH); 4.80 (*br. s*, 1 H, CH<sub>2</sub>=C); 4.96 (*br. s*, 1 H, CH<sub>2</sub>=C).

Cyclohex-2-en-1-ol (**18**). Reduction of cyclohex-2-en-2-one (*Fluka*) with CeCl<sub>3</sub>·3 H<sub>2</sub>O and NaBH<sub>4</sub> [36]. Colorless liquid. B.p. 65°/12 Torr. <sup>1</sup>H-NMR (400 MHz, CDCl<sub>3</sub>): 1.56–2.07 (*m*, 3 CH<sub>2</sub>); 4.02–4.20 (*m*, H–C(1)); 5.74–5.77 (*m*, =CH); 5.82–5.86 (*m*, =CH).

5. Enzymatic Resolution of (±)-3-Methylbut-3-en-2-ol (**16**) with Porcine Pancreatic Lipase (PPL). Following a method used for the resolution of other secondary alcohols [22], finely ground molecular sieves 4 Å (3 g) and PPL (6 g, dried 6 h at r.t. at 0.05 Torr) were added to a soln. of 2.58 g (0.03 mol) of **16** in dry methyl propionate (150 ml, *Fluka*). The suspension was magnetically stirred for 72 h at 40°, after which enzyme and molecular sieves were filtered off and washed with CH<sub>2</sub>Cl<sub>2</sub> (3 × 10 ml). After evaporation of the solvents, the propionate of (+)-**16** (1.45 g, *R<sub>f</sub>* 0.70) and the remaining alcohol (–)-**16** (1.8 g, *R<sub>f</sub>* 0.18) were separated by column chromatography (silica gel, pentane/Et<sub>2</sub>O 7:1). Propionate of (+)-**16**: <sup>1</sup>H-NMR (400 MHz, CDCl<sub>3</sub>): 1.15 (*t*, *J* = 7.7, Me); 1.32 (*d*, *J* = 6.6, Me); 1.74 (*s*, Me–C=C); 2.33 (*q*, *J* = 7.7, CH<sub>2</sub>CO), 4.84 (*br. s*, 1 H, CH<sub>2</sub>=C); 4.95 (*br. s*, 1 H, CH<sub>2</sub>=C); 5.23 (*q*, *J* = 6, CH–O).

The propionate (1.4 g) was saponified at r.t. with 1M NaOH in MeOH (30 ml) for 7 h (TLC), after which MeOH was evaporated. The residue was taken up in H<sub>2</sub>O (5 ml) and extracted with Et<sub>2</sub>O (4 × 10 ml). The extracts were dried (MgSO<sub>4</sub> and 4 Å molecular sieves) and evaporated: (+)-*R*-**16** (460 mg), 100% pure (by <sup>1</sup>H-NMR). [ $\alpha$ ]<sub>D</sub><sup>20</sup> = +5.50 (neat), [ $\alpha$ ]<sub>D</sub><sup>20</sup> = +5.77 (*c* = 8, CHCl<sub>3</sub>).

MTPA Ester of (+)-**16**. A soln. of (+)-**16** (43 mg, 0.5 mmol) in dry CH<sub>2</sub>Cl<sub>2</sub> (1 ml) was added to a soln. of (+)-(*R*)- $\alpha$ -methoxy- $\alpha$ -(trifluoromethyl)phenylacetic acid (MTPA; 129 mg, 0.55 mmol), *N,N*-dicyclohexylcarbodiimide (134 mg, 0.55 mmol) and 4-(dimethylamino)pyridine (121 mg, 0.1 mmol) in dry CHCl<sub>3</sub> (3 ml). The mixture was stirred at r.t. for ca. 4 h (TLC monitoring), filtered, washed with cold pentane (2 × 1 ml), and evaporated to give a colorless oil which was directly examined by <sup>1</sup>H- and <sup>19</sup>F-NMR: e.e. 97 ± 1%. <sup>1</sup>H-NMR (400 MHz, CDCl<sub>3</sub>): 1.35 (*d*, *J* = 5, Me); 1.74 (*s*, Me); 3.56 (*s*, MeO); 5.05 (*m*, 1 H, CH<sub>2</sub>=C); 4.93 (*m*, 1 H, CH<sub>2</sub>=C); 5.30 (*d*, *J* = 5, CH–O); 7.40–7.42 (*m*, 3 arom. H); 7.50–7.54 (*m*, 2 arom. H).

## REFERENCES

- [1] R. Gerdil, in 'Topics in Current Chemistry', Ed. E. Weber, Springer Verlag, Berlin–Heidelberg, Vol. 140, p. 75–105.
- [2] R. Gerdil, G. Barchietto, C. W. Jefford, *J. Am. Chem. Soc.* **1984**, *106*, 8004.
- [3] J. M. Thomas, J. Chen, A. George, *Chem. Br.* **1992**, 991.
- [4] M. Bartok, K. L. Lang, in 'Heterocyclic Compounds, Small Ring Heterocycles, Part 3, Oxiranes', Ed. A. Hassner, Wiley, New York, 1985, Vol. 42, p. 1–196.
- [5] B. Vierkorn-Rudolph, K. Bächmann, *Chromatographia* **1979**, *2*, 89.
- [6] R. Gerdil, G. Barchietto, *Tetrahedron Lett.* **1987**, *28*, 4685.
- [7] C. L. Kissel, B. Rickborn, *J. Org. Chem.* **1972**, *37*, 2060; M. N. Sheng, *Synthesis* **1972**, 194.
- [8] H. Yamamoto, H. Nozaki, *Angew. Chem. Int. Ed.* **1978**, *17*, 169.
- [9] H. Su, L. Walder, Z. Zhang, R. Scheffold, *Helv. Chim. Acta* **1988**, *71*, 1073; P. Bonhôte, R. Scheffold, *ibid.* **1991**, *74*, 1425.

- [10] K. Arata, K. Tanabe, *Bull. Chem. Soc. Jpn.* **1980**, *53*, 299.
- [11] R. P. Thummel, B. Rickborn, *J. Am. Chem. Soc.* **1970**, *92*, 2064.
- [12] A. C. Legon, C. A. Rego, *Angew. Chem. Int. Ed.* **1990**, *29*, 72.
- [13] G. Bernardinelli, R. Gerdil, in preparation.
- [14] H. M. Powell, in 'Non-Stoichiometric Compounds', Ed. L. Mandelcorn, Academic Press, New York, 1964, p.469; D. Lawton, H. M. Powell, *J. Chem. Soc.* **1958**, 2339.
- [15] H. C. Brown, G. G. Pai, *J. Org. Chem.* **1958**, *50*, 1387.
- [16] R. Gerdil, G. Barchietto, *Tetrahedron Lett.* **1989**, *30*, 6677.
- [17] V. Schurig, W. Bürkle, *J. Am. Chem. Soc.* **1982**, *104*, 7573; A. Gedanken, V. Schurig, *J. Phys. Chem.* **1987**, *91*, 1324.
- [18] V. Schurig, W. Bürkle, *Angew. Chem. Int. Ed.* **1978**, *17*, 132.
- [19] H. G. Lucas, H. K. Garner, *J. Am. Chem. Soc.* **1951**, *73*, 41.
- [20] K. Krassuski, *Chem. Zbl.* **1902**, *2*, 19.
- [21] D. H. G. Crout, S. M. Morrey, *J. Chem. Soc., Perkin Trans. 1* **1983**, 2435.
- [22] A. J. M. Janssen, in 'Enzymatic Resolution of Primary and Secondary Alcohols in Organic Media', Thesis, University of Nijmegen, The Netherlands, 1991, and ref. cit. therein.
- [23] A. Dale, H. S. Moscher, *J. Am. Chem. Soc.* **1973**, *95*, 512.
- [24] S. Yamada, N. Takamura, T. Mizoguchi, *Chem. Pharm. Bull.* **1975**, *23*, 2539; R. Otzet, J. Pascual, J. Sistare, *An. Real. Soc. Espan. Fis. Quim. B.* **1966**, *62*, 965.
- [25] A. C. Legon, C. A. Rego, *Angew. Chem. Int. Ed.* **1990**, *29*, 72.
- [26] D. H. Cohen, G. M. G. Schmidt, *J. Chem. Soc.* **1964**, 1996.
- [27] J. O. Trent, R. Gerdil, in preparation.
- [28] S. D. Picket, A. K. Nowak, J. M. Thomas, B. K. Paterson, J. F. P. Swift, A. K. Cheetham, C. J. J. den Ouden, B. Smit, F. M. F. Post, *J. Phys. Chem.* **1990**, *94*, 1233, and ref. cit. therein.
- [29] K. B. Wiberg, in 'Physical Organic Chemistry', John Wiley & Sons, Inc., New York, 1964.
- [30] J. M. Gnam, B. S. Green, R. Arad-Yellin, P. M. Keehn, *J. Org. Chem.* **1991**, *56*, 4525.
- [31] S. Winstein, H. J. Lucas, *J. Org. Chem.* **1939**, *61*, 1576.
- [32] C. E. Wilson, H. J. Lucas, *J. Am. Chem. Soc.* **1956**, *58*, 2396.
- [33] W. S. Johnson, D. W. Daub, T. A. Lyle, M. Niwa, *J. Am. Chem. Soc.* **1980**, *102*, 7800.
- [34] C. O. Guss, R. Rosenthal, *J. Am. Chem. Soc.* **1955**, *77*, 2549.
- [35] M. B. Green, W. J. Hickinbottom, *J. Chem. Soc.* **1957**, 3262.
- [36] A. L. Gemal, J.-L. Luche, *J. Am. Chem. Soc.* **1981**, *103*, 5454.